Journal of Alloys and Compounds 503 (2010) 519–524

Contents lists available at ScienceDirect

Journal of Alloys and Compounds

journal homepage: www.elsevier.com/locate/jallcom

Solvothermal synthesis of monodisperse self-assembly CeO_2 nanospheres and their enhanced blue-shifting in ultraviolet absorption

Bo Liu, Bingbing Liu*, Quanjun Li, Zepeng Li, Ran Liu, Xu Zou, Wei Wu, Wen Cui, Zhaodong Liu, Dongmei Li, Bo Zou, Tian Cui, Guangtian Zou

State Key Laboratory of Superhard Materials, Jilin University, Changchun 130012, PR China

ARTICLE INFO

Article history:
Received 1 March 2010
Received in revised form 5 May 2010
Accepted 8 May 2010
Available online 20 May 2010

Keywords:
Self-assembly
Solvothermal
n-Butanol
Surfactant/template-free

ABSTRACT

Monodisperse CeO_2 nanospheres with the average size of 40 nm, self-assembled by well-crystalline CeO_2 ultrafine nanoparticles were synthesized through a facile solvothermal route using n-butanol as solvent in the absence of any surfactant or template. The formation process of the monodisperse self-assembly CeO_2 nanospheres is briefly discussed. The key function of n-butanol is investigated by comparative experiments. It is found that n-butanol not only serves as solvent, but also acts as surfactant in the formation of monodisperse self-assembly CeO_2 nanospheres. Raman and XRD spectra show that the sample is pure cubic fluorite type of structure. Compared to the bulky CeO_2 materials, the prepared CeO_2 nanospheres exhibited an obvious blue-shifting in UV absorbance. The direct band gap energy of the obtained sample increases by exceeding 10%. Our study provides an effective approach to control CeO_2 morphology which has potential application in synthesis of other nanomaterials.

1. Introduction

In the past decade, extensive research efforts have been devoted to the design and preparation of nanomaterials with different shapes/sizes due to their particular shape/size-dependent properties and their promising application in electronics, optics, and magnetic [1–4]. As a well-known functional rare earth material, CeO_2 has a wide range of applications including ultraviolet (UV) blockers, abrasives, catalysts and solid oxide fuel cells [5–8].

Nanostructured CeO_2 possesses the superior physical and chemical properties compared with its bulk counterparts [9,10]. Thus, many progresses have been made in the study of the synthesis of CeO_2 nanomaterials and in the investigation of their corresponding novel properties. Up to now, well-defined CeO_2 nanostructures with various morphologies including nanoparticles [11,12], nanorods [13,14], nanoflowers [15], and hollow structures [16,17] have been successfully fabricated. Very recently, a unique morphology, self-assembly CeO_2 nanospheres which are composed of crystalline CeO_2 nanoparticles have aroused increasing attention, because they are expected to exhibit much stronger ultraviolet absorption, remarkable catalytic activity and excellent electrochemical properties as anode material in lithium ion battery. At present, fabrication of high quality self-assembly CeO_2 spherical crystallites is an important topic. Caruso et al. [18] have obtained spherical CeO_2 at micrometer scale utilizing porous polymeric beads as templates by sol–gel method. Yu and co-workers [19] have further decreased spheres size from micrometer into the range of 100 nm using PVP as the surfactant via solution method. Lately, the effective hydrothermal method has been employed in the synthesis of CeO_2 nanospheres. Zhou et al. [20] reported the size could be controlled in the range from 100 to 800 nm by PVP-assistant hydrothermal route; Shen et al. [21] employed a urea-hydrothermal route to prepare CeO_2 nanospheres with an average size of 320 nm and with a relatively narrow diameter distribution. However, to get higher specific surface area and further improve their properties, people need to further reduce their size to less than 100 nm and with a relatively narrow size distribution, more important, it is still a challenging topic to get monodisperse and highly crystalline sample for this particular material. Additionally, in the aforementioned approaches, they have been employed templates or surfactants to control the morphology and in most of cases, further calcination treatment is usually inevitable. Therefore, it is necessary to avoid employing other additives in the synthesis process and to find a new straightforward and general approach in synthesis of monodisperse CeO_2 spherical nanocrystallites with smaller sizes by one step.

As a facile and effective technique, solvothermal method instead of hydrothermal process has been widely employed in the synthesis of various nanomaterials due to its extraordinary advantages of one-step synthesis, controllable dispersion and crystallization [22–25]. Recently, it has been found that adopting appropriate alcohol in solvothermal process could tailor the shape and size

* Corresponding author. Tel.: +86 431 85168256; fax: +86 431 85168256.
E-mail address: liubb@jlu.edu.cn (B. Liu).

0925-8388/$ – see front matter.
doi:10.1016/j.jallcom.2010.05.047

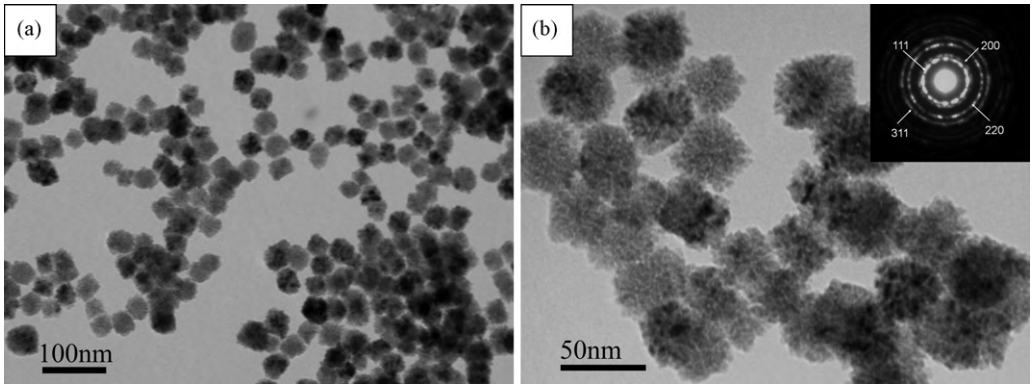

Fig. 1. TEM micrographs and ED pattern of the typical product: (a) low magnification image; (b) high magnification image and ED pattern (inset).

of nanostructures without any other additives. For instance, Yang et al. [26] fabricated highly crystalline and monodisperse TiO_2 nanocubes of pure anatase phase in an n-butanol system; Ma et al. [27] even prepared column-like ZnO microcrystals with various sizes by utilizing different alcohols as solvents. Their studies motivated us to synthesize self-assembly CeO_2 nanospheres by using solvothermal method with alcohols as solvents. In addition, it should be pointed out how these alcohols influence the morphology and the formation mechanism are open questions so far. Thus, our study also helps us to understand the effect of alcohol in the formation of nanomaterials with various morphologies.

In the present work, we report the first study on the synthesis of monodisperse self-assembly CeO_2 nanospheres with an average size of 40 nm, aggregated by well crystallization nanoparticles using solvothermal method adopting n-butanol as solvent, without any other additives. The as-prepared nanospheres have been characterized by transmission electron microscopy (TEM), X-ray diffraction (XRD), Raman spectroscopy, FTIR spectroscopy and UV–vis spectroscopy. It is found that our sample has strong UV absorption and exhibited an obvious blue-shifting. The effect of n-butanol in the formation of CeO_2 nanospheres has been investigated by adjusting the volume ratio of ethylene glycol to n-butanol. We found that n-butanol is not only employed as solvents in the formation process but also serves as surfactant which plays an important role in the formation of self-assembly CeO_2 nanospheres. Our study provides an effective approach to control CeO_2 morphology which has potential application in synthesis of other nanomaterials.

2. Experimental details

All the reactants used were analytical grade without any further purification before the experiment. A Teflon-lined stainless steel cylindrical closed chamber with 50 mL capacity was used to synthesize the CeO_2 nanocrystals in the following detailed process. In a typical synthesis, 1 mmol $Ce(NO_3)_3{\cdot}6H_2O$ was loaded into the Teflon-lined chamber which was filled to 80% of its total capacity with 40 mL n-butanol. After being fully stirred to obtain a transparent solution, the autoclave was sealed and put into an oven which was maintained at 120 °C for 15 h and then cooled to room temperature naturally. The resulting yellow precipitates were separated by centrifuging, washed with ethanol and distilled water several times, respectively. Then, the final product was dried in air at 60 °C for 12 h and was collected for further characterization.

The (HITACHI H-8100) transmission electron microscope (TEM) with accelerator voltage of 200 kV was employed to observe the morphology of the product. X-ray powder diffraction (XRD) was used to characterize the product with Cu Kα radiation (λ = 0.15418 nm). When characterized by XRD, a scanning rate of 0.02° s^{-1} was applied and the scanning range is 10–90°. Raman spectrum was excited by radiation of 514.5 nm from a Renishaw inVia Raman spectrometer. FTIR spectrum was obtained on Bruker FTPL (Vertex 80V) FTIR spectrometer with a resolution of 4 cm^{-1}. The UV–vis spectrum of the product was recorded on a UV-3150 spectrophotometer using a quartz cell (1 cm path length). The as-prepared powder was dispersed in ethanol at a concentration of around 0.2 g L^{-1} and then sonicated at room temperature for 10 min to obtain a transparent colloidal solution. Ethanol was taken into account for blank. The optical absorption coefficient α was calculated according to the following equation: $\alpha = 2303A\rho/lc$, where A is the absorbance of the sample, ρ is the real density of CeO_2 (7.28 g cm^{-3}), l is the path length of the quartz cell (1 cm), and c is the concentration of the ceria suspensions [28]. The product for UV–vis spectrum was calcined at 500 °C for 2 h in order to removing the residual organic reagent. The product maintained its original morphology after calcination.

3. Results and discussion

The morphology and structure of the self-assembly CeO_2 nanospheres were characterized by TEM and electron diffraction (ED) technique. The representative TEM micrographs of the typical product are shown in Fig. 1(a) and (b). These graphs reveal that all of the synthesized CeO_2 nanocrystals are monodisperse CeO_2 nanospheres with an average size of 40 nm and a narrow diameter distribution. Comparing with the previous works, it is clearly seen that the as-prepared CeO_2 nanospheres exhibit much smaller size and finer dispersion [19,20]. High magnification image (Fig. 1(b)) reveals a clear grain boundary on the product surface, indicating that the as-fabricated CeO_2 nanospheres are assembled by crystalline CeO_2 nanoparticles. The size of the compositive ultrafine CeO_2 nanoparticles is in the range of 3–8 nm. ED pattern (inset in Fig. 1(b)) determines the polycrystalline nature of the product and well crystalline with cubic fluorite structure without further calcination.

To precisely determine the crystal structure of the as-prepared sample, we carried out XRD analysis. Fig. 2 exhibits the XRD pattern of the self-assembly CeO_2 nanospheres. All the detectable peaks in the pattern can be indexed to the pure cubic fluorite CeO_2 with a lattice constant $a = 0.5420(2)$ nm (JCPDS Card NO. 81-0792).

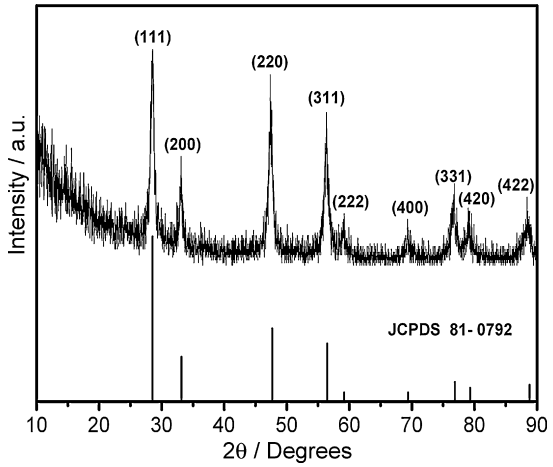

Fig. 2. XRD pattern of the self-assembly CeO_2 nanospheres.

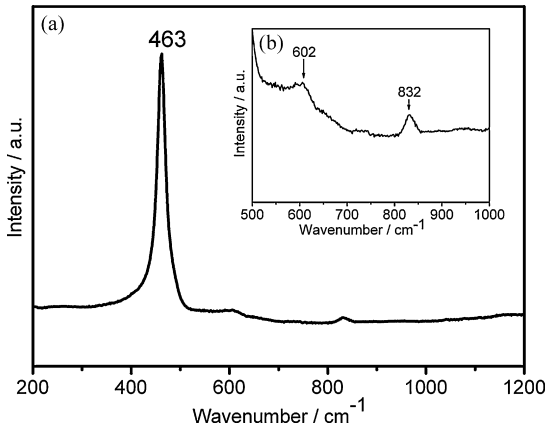

Fig. 3. (a) Raman spectrum of the synthesized CeO_2 nanospheres; (b) the second order Raman peaks of the synthesized CeO_2 nanospheres.

This value is in good agreement with the result for the previous study of nanoparticles with the size of 4.7 nm [28]. According to Debye–Scherrer formula, the strongest peak (1 1 1) at $2\theta = 28.535^\circ$, the peak (2 0 0) at $2\theta = 33.062^\circ$, the peak (2 2 0) at $2\theta = 47.368^\circ$ and the peak (3 1 1) at $2\theta = 56.230^\circ$ are used to calculated the average particle size of the self-assembly CeO_2 nanospheres, determined to be around 5 nm. These results are consistent with that obtained by TEM and ED analysis. No impurity was detected from the XRD spectrum, indicating that the self-assembly CeO_2 nanospheres with high purity could be prepared by the current synthetic system.

In order to further confirm the formation of the cubic structure in the synthesized CeO_2 nanospheres, Raman spectroscopy was also performed. Raman spectrum of the synthesized CeO_2 nanospheres is shown in Fig. 3(a). CeO_2 with cubic fluorite type of structure belongs to the $O_h^5(Fm3m)$ space group [29]. The typical sample exhibits only one first order Raman peak ($\sim$463 cm^{-1}) in the spectrum, which can be assigned to F_{2g} symmetry as a symmetrical stretching mode of the Ce–8O vibrational units. The second order Raman peaks (shown in Fig. 3(b)) for the CeO_2 nanospheres are 602, 832 cm^{-1}. These results are consistent with the previous studies of the pure cubic fluorite CeO_2 nanomaterials [30].

To investigate the formation process of the self-assembly CeO_2 nanospheres, samples were collected at different reaction times and were characterized by the TEM and ED analysis. Fig. 4 shows the TEM images and ED patterns of the samples collected at different reaction times. These images clearly reveal the evolution from nanoparticles to nanospheres. At the initial stage, it is obvious that the small nanoparticles are mainly produced in the reaction system (Fig. 4(a)). When increasing the reaction time to 5 h, the spherical crystals emerged but aggregated with the size about 20 nm (Fig. 4(b)). With further increasing the reaction time, the size of the nanospheres increases obviously and the dispersion of the nanospheres are well improved (Fig. 4(c)). When the reaction time is 15 h, the monodisperse self-assembly CeO_2 nanospheres are successfully obtained, and the size increases finally to 40 nm (Fig. 4(d)). Particularly, it is noticed that ED patterns (inset in Fig. 4) show all the samples are ceria crystals with cubic fluorite crystal structure in all reaction stages. This result is contrast to previous studies, in which cerium precursors such as metal alkoxide, cerium hydroxide carbonate and cerium format were usually formed and calcination was thus necessary for the formation of ceria with two steps [19,31,32]. Therefore, our study clearly reveals that the evolution from CeO_2 nanoparticles to monodisperse self-assembly CeO_2 nanospheres is a one-step process.

Based on the above results, the formation of monodisperse CeO_2 nanospheres might be explained by a self-assembly process of the metastable aggregated particles. Similar evolution process has been presented in the synthesis of TiO_2, SnO_2, etc. [33,34]. Here we propose the process of the formation of CeO_2 nanospheres shown in Fig. 5. In the early stage of the synthetic process, ceria can be formed easily. The newly formed CeO_2 nanoparticles have high surface

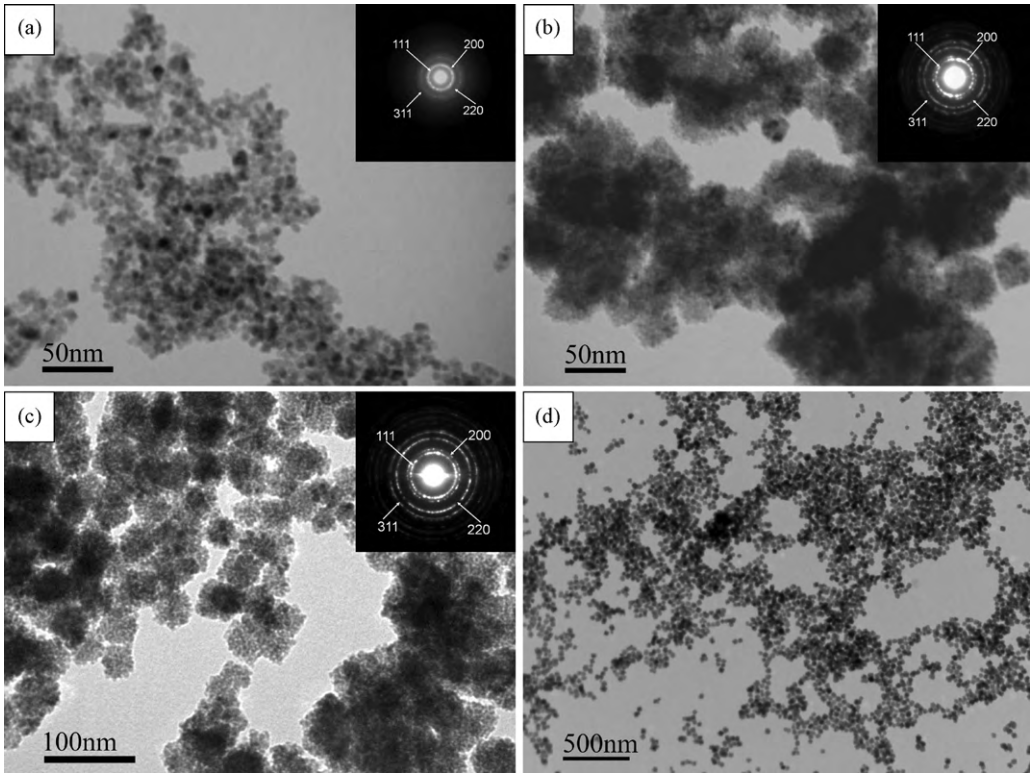

Fig. 4. TEM images and ED patterns (inset) of the samples collected at different reaction times: (a) 1 h; (b) 5 h; (c) 10 h; (d) 15 h.

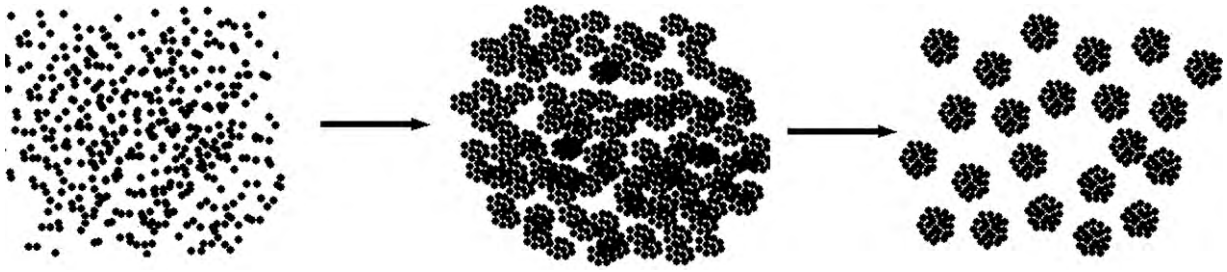

Fig. 5. Schematic illustration of the formation of CeO_2 nanospheres.

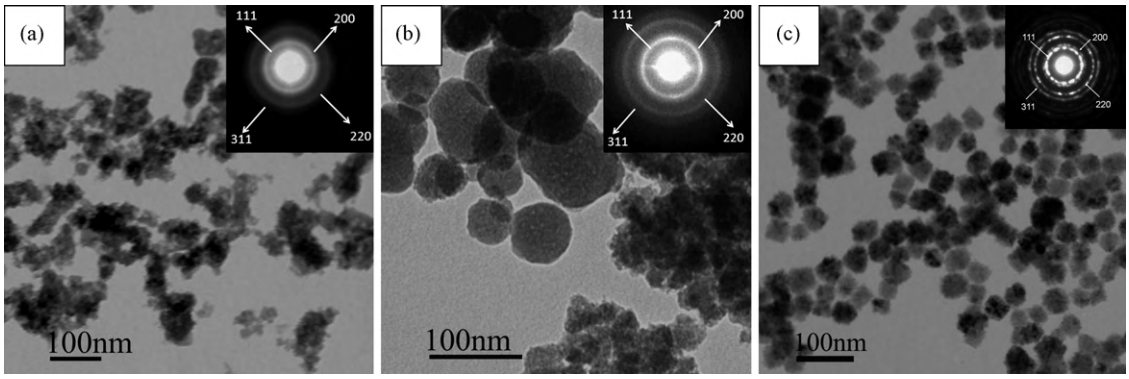

Fig. 6. TEM images and ED patterns (inset) of CeO_2 samples using different solvents: (a) ethylene glycol; (b) a mixture of n-butanol and ethylene glycol in 1:1 volume ratio; (c) n-butanol.

energy, which make them highly reactive, and tend to aggregate into bigger crystals to reduce their surface energy and to reach a thermodynamically equilibrium status. In our synthetic route, the application of n-butanol plays an important role in the formation of the monodisperse self-assembly CeO_2 nanospheres. To Figure out the effect of n-butanol, comparative experiments were carried out. In previous studies, ethylene glycol has been extensively adopted to prepare inorganic metallic oxide in solvothermal synthetic systems due to its strong reducing powder and relatively high boiling point [35]. In particular, spherical cobalt has been successfully prepared in PVP-assistant solvothermal process adopting ethylene glycol as solvent [36]. We thus investigated the function of n-butanol using ethylene glycol as solvent in solvothermal process. The effect of n-butanol in the formation of CeO_2 nanospheres was investigated by adjusting the volume ratio of ethylene glycol to n-butanol. In comparative experiment (1), ethylene glycol is used instead of n-butanol, and other synthetic parameters are kept the same as these in the typical synthesis. The resulting product exhibits random agglomeration without the assistance of n-butanol (Fig. 6(a)). In comparative experiment (2), a mixture of n-butanol and ethylene glycol 1:1 volume ratio is selected as solvent, while other synthetic parameters are unchanged. It is obvious that the mainly product is spherical morphology and is well dispersed under the assistance of n-butanol (Fig. 6(b)). Attractively, when pure n-butanol was used as solvent, only monodisperse CeO_2 nanospheres are produced (Fig. 6(c)). ED patterns (inset in Fig. 6(a) to 6(c)) confirm all the products are cubic fluorite type CeO_2.

To further figure out the effect of n-butanol on the formation of monodisperse self-assembly CeO_2 nanospheres, FTIR spectrum of the typical sample was carried out. Fig. 7 shows the IR spectrum of the synthesized CeO_2 nanospheres. The typical peaks of n-butanol and CeO_2 are clearly exhibited in Fig. 7. Three peaks at 2970, 2930 and 2874 cm^{-1} are characteristic of C-H stretching modes for CH_2 and CH_3 groups and the peaks at 1087 and 1052 cm^{-1} are characteristic of C–OH stretching modes for alcohol. These typical peaks indicate that the sample is coated by n-butanol [37,38]. Attractively, the peak located at 480 cm^{-1} owing to Ce–O stretching band exhibits great shifting than previous reports [19,39]. The above results strongly exhibit the modification of n-butanol. In addition, the peaks at 2361 and 2341 cm^{-1} attribute to CO_2. The peak at ca. 3400, 1645, 1540 and 1436 cm^{-1} correspond to the water on the sample [38–40].

The above analysis clearly validates the important role of n-butanol in the formation of monodisperse self-assembly CeO_2 nanospheres. Under the modification of n-butanol, the random aggregation is avoided. With increasing the volume radio of n-butanol, the morphology and dispersion of the product are well improved owning to the steric effect of n-butanol [41]. Therefore, comparing the effect of PVP in the formation of spherical structures [36], a possible function of n-butanol can be proposed as follows: n-butanol may serve as not only solvent but also surfactant in our solvothermal synthesis.

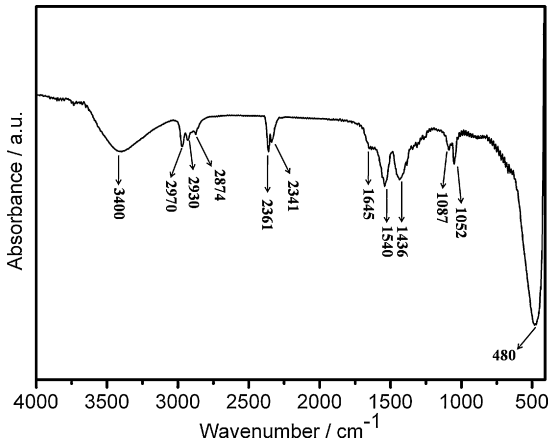

Fig. 7. FTIR spectrum of the typical sample.

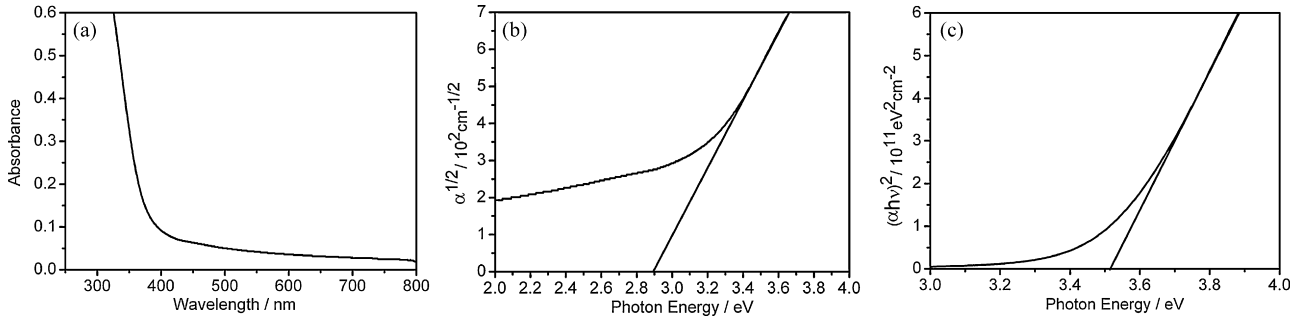

Fig. 8. (a) UV spectrum for annealed CeO_2 nanospheres; (b) plot of $\alpha^{1/2}$ vs photon energy for annealed CeO_2 nanospheres; (c) plot of $(\alpha h\upsilon)^2$ vs photon energy for annealed CeO_2 nanospheres.

Optical properties of the typical sample were characterized by UV absorption spectrum. Fig. 8(a) shows the typical absorption spectrum of the synthesized CeO_2 nanospheres. A strong blue-shifting absorption below 400 nm can be observed for the typical sample, which originates from charge-transfer between the O 2p and Ce 4f states in O^{2-} and Ce^{4+} [42,43]. For indirect interband transitions, α near the absorption edge can be expressed in the following equation [44]:

$$\frac{\alpha \propto (h\upsilon + E_p - E_i)^2}{(e^{h\upsilon/\kappa T} - 1)} + \frac{(h\upsilon - E_p - E_i)^2 e^{h\upsilon/\kappa T}}{(e^{h\upsilon/\kappa T} - 1)}$$

where E_i is the band gap energy for indirect transitions and E_p is the phonon energy, κ is Boltzmann constant, and T is the absolute temperature. The plot of $\alpha^{1/2}$ vs photon energy of CeO_2 nanospheres is shown in Fig. 8(b). The intersection of the extrapolated linear portion gives the indirect band gap energy (E_i). The E_i value of the CeO_2 nanospheres was obtained as 2.89 eV. The value is consistent with the previous study of CeO_2 nanoparticles [44].

For direct transitions, α near the absorption edge can be expressed in the following equation [44]:

$$\alpha \propto \frac{(h\upsilon - E_d)^{1/2}}{h\upsilon}$$

where E_d is the band gap energy for direct transitions and $h\upsilon$ is photon energy. The plot of $(\alpha h\upsilon)^2$ vs photon energy of the CeO_2 nanospheres is shown in Fig. 8(c). From the intersection of the extrapolated linear portion, the E_d value of the CeO_2 nanospheres was determined as 3.51 eV. Compared to the pure bulk crystal (E_d = 3.19 eV) [45], the direct band gap energy of the CeO_2 nanospheres increases by exceeding 10%. By contrast, the previous studies of the CeO_2 nanospheres with the average size about 100 nm, the direct band gap energy was 3.46 eV, due to the quantum size effect [19]. The larger blue-shifting of the obtained CeO_2 nanospheres in our work may be contributed to the smaller size of the building units. Therefore, the synthesized self-assembly CeO_2 nanospheres with excellent performance for UV absorption are eminent materials that can prevent some damage from ultraviolet rays. Additionally, the obtained sample combined with other CeO_2 nanomaterials exhibiting different absorption edges could adjust the absorption of light in UV region.

4. Conclusions

In summary, we have synthesized monodisperse CeO_2 nanospheres self-assembled by well-crystalline CeO_2 ultrafine nanoparticles, with an average diameter of 40 nm via a facile solvothermal method using n-butanol as the solvent without any surfactant or template. The formation process of the monodisperse self-assembly CeO_2 nanospheres is briefly discussed. The key function of n-butanol is investigated by comparative experiments. It is found that n-butanol not only serves as solvent, but also acts as surfactant in the formation of monodisperse self-assembly CeO_2 nanospheres. With the modification and steric effect of n-butanol, CeO_2 nanoparticles aggregated to highly compacted nanospheres. Raman and XRD spectra show that the sample is pure cubic fluorite type of structure. Compared with the bulk materials, the blue-shifting in the UV absorption spectra was clearly observed for the obtained CeO_2 nanospheres. The direct band gap energy of the obtained sample increases by exceeding 10%. The excellent performance for UV absorption makes the sample an optimal candidate that can prevent the damage from ultraviolet rays.

Acknowledgements

This work was supported financially by the NSFC (10979001), the National Basic Research Program of China (2005CB724400), the Program for the Changjiang Scholar and Innovative Research Team in University (IRT0625), the Cheung Kong Scholars Programme of China, and the National Fund for Fostering Talents of Basic Science (J0730311).

References

[1] Y. Liu, K. Zhong, K. Luo, M. Gao, H. Pan, Q. Wang, J. Am. Chem. Soc. 131 (5) (2009) 1862–1870.
[2] Y. Xia, P. Yang, Y. Sun, Y. Wu, B. Mayers, B. Gates, Y. Yin, F. Kim, H. Yan, Adv. Mater. 15 (5) (2003) 353–389.
[3] Z.L. Wang, Z.W. Quan, P.Y. Jia, C.K. Lin, Y. Luo, Y. Chen, J. Fang, W. Zhou, C.J. O'Connor, J. Lin, Chem. Mater. 18 (8) (2006) 2030–2037.
[4] Y. Zhou, J. Lin, S. Wang, J. Solid State Chem. 171 (1–2) (2003) 391–395.
[5] X. Lu, X. Li, F. Chen, C. Ni, Z. Chen, J. Alloys Compd. 476 (1–2) (2009) 958–962.
[6] R. Ran, Y. Guo, Y. Zheng, K. Wang, Z. Shao, J. Alloys Compd. 491 (1–2) (2010) 271–277.
[7] S. Li, Z. Li, B. Bergmana, J. Alloys Compd. 492 (1–2) (2010) 392–395.
[8] S. Kim, J.S. Lee, C. Mitterbauer, Q.M. Ramasse, M.C. Sarahan, N.D. Browning, H.J. Park, Chem. Mater. 21 (7) (2009) 1182–1186.
[9] S.A. Hassanzadeh-Tabrizi, M. Mazaheri, M. Aminzareb, S.K. Sadrnezhaad, J. Alloys Compd. 491 (1–2) (2010) 499–502.
[10] J. Lee, J.-P. Ahn, S.W. Kim, J. Nanosci. Nanotechnol. 10 (2010) 130–134.
[11] Y.-P. Fu, C.-H. Lin, C.-S. Hsu, J. Alloys Compd. 391 (1–2) (2005) 110–114.
[12] Z.L. Wang, X. Feng, J. Phys. Chem. B 107 (49) (2003) 13563–13566.
[13] A. Vantomme, Z.-Y. Yuan, G. Du, B.-L. Su, Langmuir 21 (3) (2005) 1132–1135.
[14] H.-X. Mai, L.-D. Sun, Y.-W. Zhang, R. Si, W. Feng, H.-P. Zhang, H.-C. Liu, C.-H. Yan, J. Phys. Chem. B 109 (51) (2005) 24380–24385.
[15] C. Sun, H. Li, L. Chen, J. Phys. Chem. Solids 68 (9) (2007) 1785–1790.
[16] G. Chen, C. Xu, X. Song, S. Xu, Y. Ding, S. Sun, Cryst. Growth Des. 8 (12) (2008) 4449–4453.
[17] Y. Zhang, T. Cheng, Q. Hu, Z. Fang, K. Han, J. Mater. Res. 22 (6) (2007) 1472–1478.
[18] D.G. Shchukin, R.A. Caruso, Chem. Mater. 16 (11) (2004) 2287–2292.
[19] C. Ho, J.C. Yu, T. Kwong, A.C. Mak, S. Lai, Chem. Mater. 17 (17) (2005) 4514–4522.
[20] F. Zhou, X. Zhao, H. Xu, C. Yuan, J. Phys. Chem. C 111 (4) (2007) 1651–1657.
[21] N. Ta, M. Zhang, J. Li, H. Li, Y. Li, W. Shen, Chin. J. Catal. 29 (11) (2008) 1070–1072.
[22] Z. Li, B. Liu, X. Li, S. Yu, L. Wang, Y. Hou, Y. Zou, M. Yao, Q. Li, B. Zou, T. Cui, G. Zou, G. Wang, Y. Liu, Nanotechnology (25) (2007) 255602.
[23] J. Xu, J.-P. Ge, Y.-D. Li, J. Phys. Chem. B 110 (6) (2006) 2497–2501.
[24] J. Yang, C. Li, Z. Quan, D. Kong, X. Zhang, P. Yang, J. Lin, Cryst. Growth Des. 8 (2) (2008) 695–699.
[25] B. Wen, Y. Huang, J.J. Boland, J. Phys. Chem. C 112 (1) (2008) 106–111.

[26] X. Yang, H. Konishi, H. Xu, M. Wu, Eur. J. Inorg. Chem. 2006 (11) (2006) 2229–2235.
[27] J. Ma, C. Jiang, Y. Xiong, G. Xu, Powder Technol. 167 (1) (2006) 49–53.
[28] Y.-W. Zhang, R. Si, C.-S. Liao, C.-H. Yan, C.-X. Xiao, Y. Kou, J. Phys. Chem. B 107 (37) (2003) 10159–10167.
[29] G.A. Kourouklis, A. Jayaraman, G.P. Espinosa, Phys. Rev. B 37 (8) (1988) 4250–4253.
[30] J.E. Spanier, R.D. Robinson, F. Zhang, S.-W. Chan, I.P. Herman, Phys. Rev. B 64 (24) (2001), 245407-1-8.
[31] L.-S. Zhong, J.-S. Hu, A.-M. Cao, Q. Liu, W.-G. Song, L.-J. Wan, Chem. Mater. 19 (7) (2007) 1648–1655.
[32] Z. Guo, F. Du, G. Li, Z. Cui, Inorg. Chem. 45 (10) (2006) 4167–4169.
[33] R.L. Penn, J.F. Banfield, Science 281 (5379) (1998) 969–971.
[34] H.G. Yang, H.C. Zeng, Angew. Chem. Int. Ed. 43 (44) (2004) 5930–5933.
[35] M. Wei, H. Zhou, Y. Konishi, M. Ichihara, H. Sugiha, H. Arakawa, Inorg. Chem. 45 (14) (2006) 5684–5690.
[36] Y.-J. Zhang, Q. Yao, Y. Zhang, T.-Y. Cui, D. Li, W. Liu, W. Lawrence, Z.-D. Zhang, Cryst. Growth Des. 8 (9) (2008) 3206–3212.
[37] X. Lu, K.J. Ziegler, A. Ghezelbash, K.P. Johnston, B.A. Korgel, Nano Lett. 4 (5) (2004) 969–974.
[38] S.F. Weng, Fourier Transform Infrared Spectroscopy, Chemical Industry Press, Beijing, 2005, p. 325.
[39] S. Phoka, P. Laokul, E. Swatsitang, V. Promarak, S. Seraphin, S. Maensiri, Mater. Chem. Phys. 115 (1) (2009) 423–428.
[40] S.-Y. Wu, H.-S. Hsueh, M.H. Huang, Chem. Mater. 19 (24) (2007) 5986–5990.
[41] J. Liu, W. Qin, S. Zuo, Y. Yu, Z. Hao, J. Hazard. Mater. 163 (1) (2009) 273–278.
[42] S. Tsunekawa, R. Sahara, Y. Kawazoe, A. Kasuya, Mater. Trans. JIM 41 (8) (2000) 1104–1107.
[43] Z. Wang, Z. Quan, J. Lin, Inorg. Chem. 46 (13) (2007) 5237–5242.
[44] T. Masui, K. Fujiwara, K.-i. Machida, G.-y. Adachi, T. Sakata, H. Mori, Chem. Mater. 9 (10) (1997) 2197–2204.
[45] S. Tsunekawa, T. Fukuda, A. Kasuya, J. Appl. Phys. 87 (3) (2000) 1318–1321.